Cell Reports, Volume *16*

Supplemental Information

PML at Mitochondria-Associated Membranes Is Critical for the Repression of Autophagy and Cancer Development

Sonia Missiroli, Massimo Bonora, Simone Patergnani, Federica Poletti, Mariasole Perrone, Roberta Gafà, Eros Magri, Andrea Raimondi, Giovanni Lanza, Carlo Tacchetti, Guido Kroemer, Pier Paolo Pandolfi, Paolo Pinton, and Carlotta Giorgi

SUPPLEMENTAL DATA ITEMS

Supplemental figures and legends

Figure S1

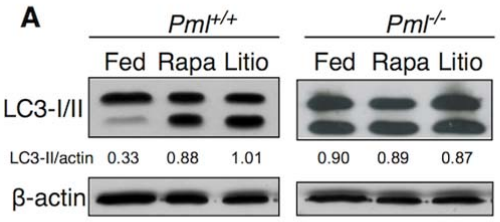

B

Quantification normalized on Sigma 1-R			
MAMs	*Pml*$^{+/+}$	*Pml*$^{-/-}$	% of increase $^{-/-}$ v $^{+/+}$
ATG14	0.11	0.25	127.27%
STX17	0.26	0.58	123.07%

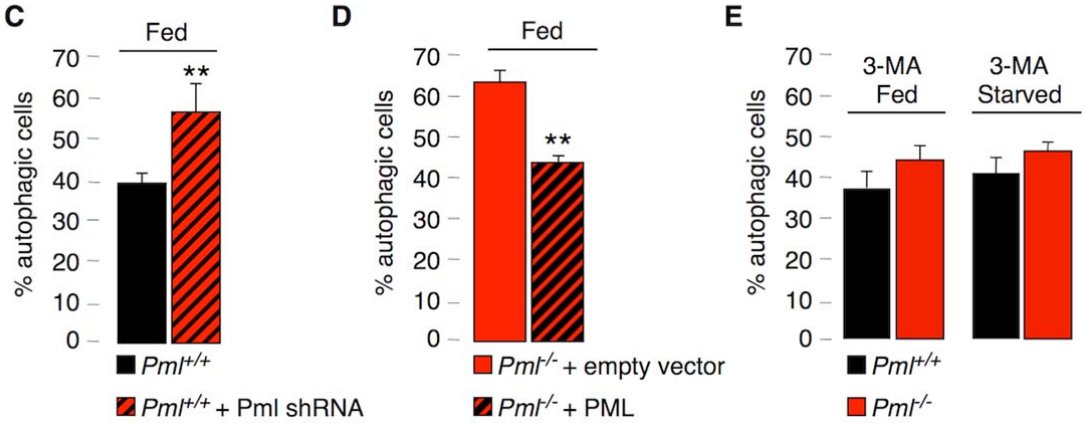

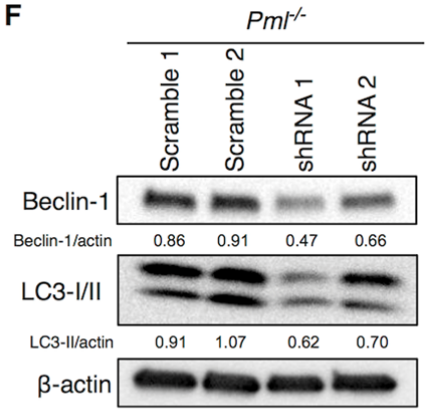

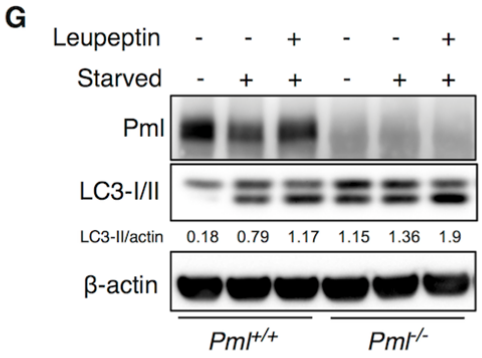

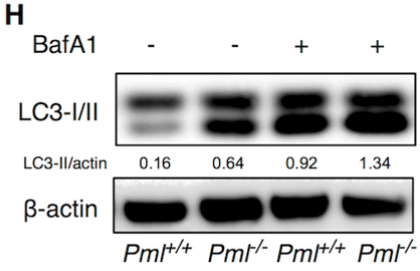

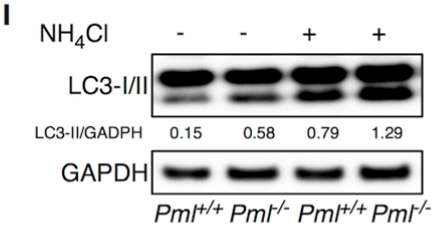

Figure S1, Related to Figure 1. High levels of autophagy under PML KO conditions, either *in vitro* or *in vivo*.
(A) Induction of LC3-I lipidation following treatment with rapamycin (100 nM, 24 h) and lithium (10 mM, 24 h) in $Pml^{+/+}$ and $Pml^{-/-}$ MEFs.
(B) ATG14 and STX17 protein quantification at MAM regions normalized to the amount of Sigma 1-R.
(C-D) Formation of GFP-LC3 puncta under (C) Pml shRNA conditions or (D) after the re-introduction of PML into $Pml^{-/-}$ MEFs. Bars: S.E.M. ** $p < 0.01$, n=3.
(E) Percentage of GFP-LC3 puncta-positive cells (MEFs) after 3-MA (10 mM, 3 h) treatment under fed and starved conditions (serum deprivation, 1 h). Bars: S.E.M.
(F) Reduced levels of autophagy in $Pml^{-/-}$ MEFs after Beclin-1 silencing.
(G) *In vivo* autophagic flux assessed by immunoblot for endogenous LC3 in $Pml^{+/+}$ and $Pml^{-/-}$ mice liver after leupeptin treatment (Esteban-Martinez and Boya, 2015).
(H) Accumulation of LC3-II obtained by interrupting the autophagosome-lysosome fusion step with bafilomycin A1 in MEF cells (Klionsky et al., 2016).
(I) LC3 turnover assay to measure the autophagic flux in MEFs cultured in the presence of ammonium chloride (NH_4Cl).

Figure S2

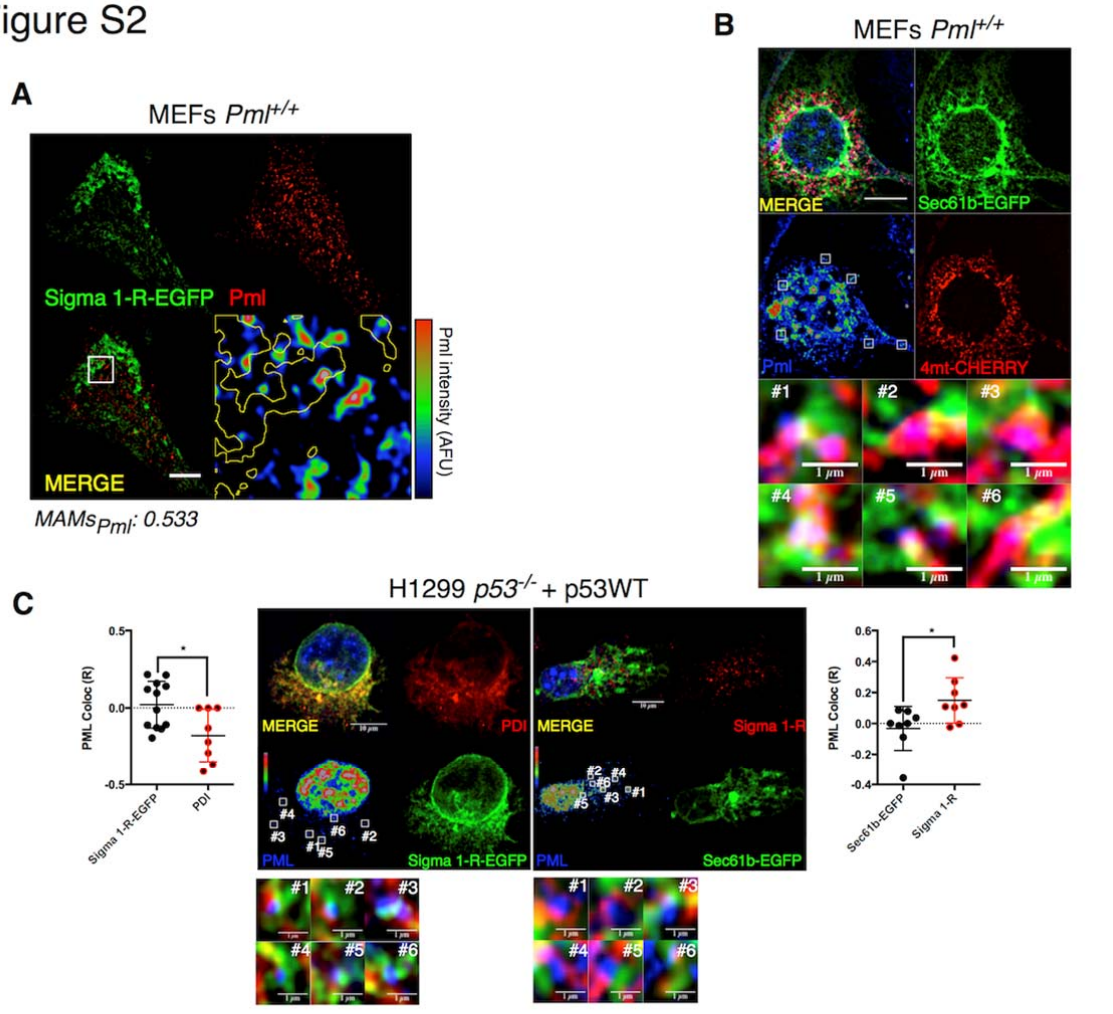
A
MEFs Pml+/+
Sigma 1-R-EGFP
Pml
MERGE
Pml intensity (AFU)
MAMsPml: 0.533
B
MEFs Pml+/+
MERGE
Sec61b-EGFP
Pml
4mt-CHERRY
#1
#2
#3
#4
#5
#6
C
H1299 p53-/- + p53WT
PML Coloc (R)
Sigma 1-R-EGFP
PDI
MERGE
PDI
PML
Sigma 1-R-EGFP
MERGE
Sigma 1-R
PML
Sec61b-EGFP
PML Coloc (R)
Sec61b-EGFP
Sigma 1-R

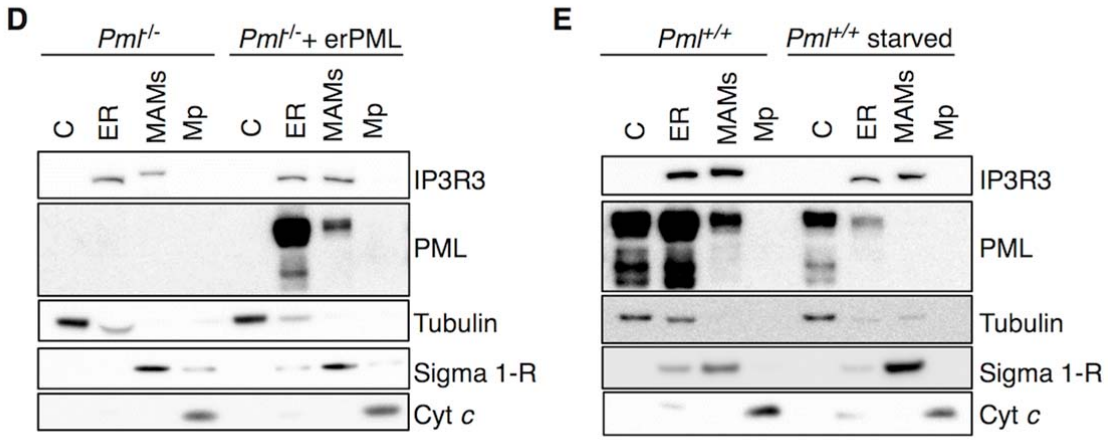
D
Pml-/-
Pml-/-+ erPML
C
ER
MAMs
Mp
IP3R3
PML
Tubulin
Sigma 1-R
Cyt c
E
Pml+/+
Pml+/+ starved
C
ER
MAMs
Mp
IP3R3
PML
Tubulin
Sigma 1-R
Cyt c

Figure S2, Related to Figure 2. Proper localization of PML at ER/MAM contact sites is fundamental to inducing autophagy.

(A) Representative confocal images of Sigma 1-R-EGFP (green) and Pml (red) in WT MEFs. The lower left panel displays the merged image of the two stains. The lower right panel displays the Pml signal overlaid with MAMs in a rainbow LUT (*$MAMs_{PML}$:* Manders coefficient for Pml staining was calculated according to Manders coefficient method as the proportion of Pml signal overlapping with the Sigma 1-R marker). Scale bar, 10 μm.

(B) Representative confocal immunofluorescence of Pml (rainbow LUT) in *$Pml^{+/+}$* MEFs expressing the mitochondrial marker 4mt-Cherry and the ER marker Sec61b-EGFP (green). Scale bar, 10 μm. On right side zoomed regions of close contacts of Pml signal together with ER and mitochondria markers (scale bar, 1 μm). Relative inset are displayed on Pml image.

(C) Representative confocal immunofluorescence of PML (rainbow LUT) and PDI (red, left panel) or Sigma 1-R (red, right panel) in H1299 cells reintroduced of $p53^{wt}$ and co-expressing Sigma 1-R-EGFP (green, left panel) or Sec61b-EGFP (green, right panel). Scale bar, 10 μm. On bottom, zoomed regions of close contacts of PML signal together with ER and MAMs markers (scale bar, 1 μm). Relative inset are displayed on PML image. Quantitative measurements of colocalization between Pml and ER or MAM marker are displayed beside each marker combination. Bars: S.E.M. * $p < 0.01$., n=3.

(D) Localization of Pml as detected *via* immunoblotting following subcellular fractionation in *$Pml^{-/-}$* MEFs transfected with erPML. C: cytosol; ER: endoplasmic reticulum; MAMs: mitochondria-associated membranes; Mp: pure mitochondria.

(E) Delocalization of Pml away from the MAM fraction in *$Pml^{+/+}$* MEF cells under starvation conditions (1 h). C: cytosol; ER: endoplasmic reticulum; MAMs: mitochondria-associated membranes; Mp: pure mitochondria.

Figure S3

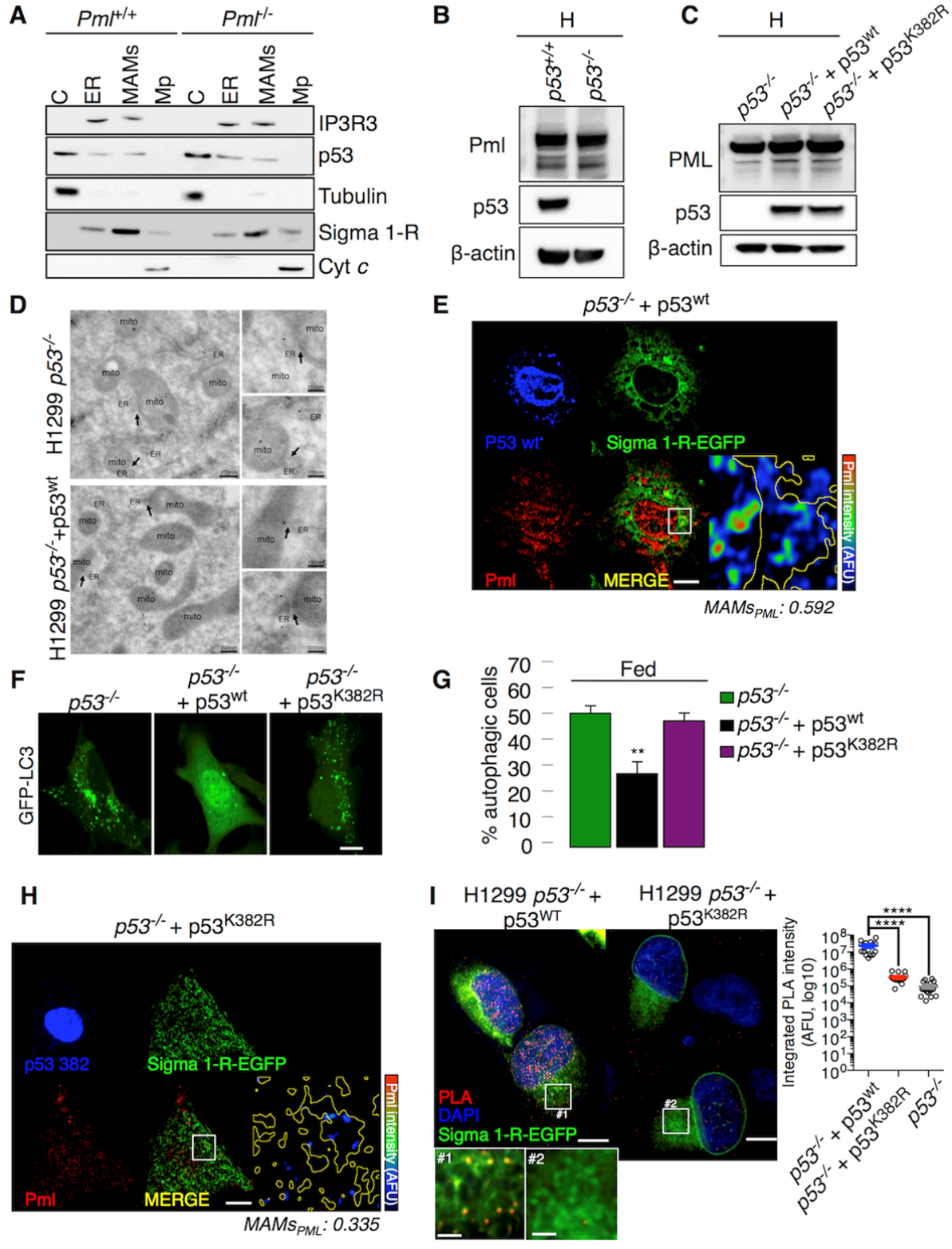
A
Pml+/+
Pml-/-
C
ER
MAMs
Mp
IP3R3
p53
Tubulin
Sigma 1-R
Cyt c
B
H
p53+/+
p53-/-
Pml
p53
β-actin
C
H
p53-/-
p53-/- + p53wt
p53-/- + p53K382R
PML
p53
β-actin
D
H1299 p53-/-
H1299 p53-/-+p53wt
mito
ER
E
p53-/- + p53wt
P53 wt
Sigma 1-R-EGFP
Pml
MERGE
Pml intensity (AFU)
MAMsPML: 0.592
F
p53-/-
p53-/- + p53wt
p53-/- + p53K382R
GFP-LC3
G
Fed
% autophagic cells
70
60
50
40
30
20
10
0
**
p53-/-
p53-/- + p53wt
p53-/- + p53K382R
H
p53-/- + p53K382R
p53 382
Sigma 1-R-EGFP
Pml
MERGE
Pml intensity (AFU)
MAMsPML: 0.335
I
H1299 p53-/- + p53WT
H1299 p53-/- + p53K382R
PLA
DAPI
Sigma 1-R-EGFP
#1
#2
Integrated PLA intensity (AFU, log10)
****
****
p53-/- + p53wt
p53-/- + p53K382R
p53-/-

Figure S3, Related to Figure 3. A p53 WT is essential for PML localization at ER/MAM contact sites and its autophagy modulation.

(A) Localization of p53 as detected via immunoblotting following subcellular fractionation in $Pml^{+/+}$ and $Pml^{-/-}$ MEFs. C: cytosol; ER: endoplasmic reticulum; MAMs: mitochondria-associated membranes; Mp: pure mitochondria. p53 immunoblot was obtained after antibodies stripping of STX17 lane from Figure 1F. Tubulin immunoblot was obtained after antibodies stripping of p53 lane from this figure.

(B) Immunoblotting of Pml levels in $p53^{+/+}$ and $p53^{-/-}$ MEFs. H: total homogenate.

(C) Immunoblotting of PML levels in $p53^{-/-}$ H1299 following the re-introduction of $p53^{wt}$ or mutant $p53^{K382R}$. H: total homogenate.

(D) Immunogold labeling of cryosections for PML. Representative images of the localization of PML in H1299 p53WT and $p53^{-/-}$ cells. Colloidal gold particles (10 nm) are associated with the ER, outer mitochondria membranes and MAMs (arrows) in p53 expressing cells. In H1299 $p53^{-/-}$ the labeling is still present on ER membranes but excluded from mitochondria or MAMs (arrows). Scale bar: left panel 1 μm, upper right panel 500 nm and lower right panel 250 nm.

(E) Immunofluorescence of Pml (red) and p53 (blue) in $p53^{-/-}$ MEFs after the re-introduction of $p53^{wt}$. Sigma 1-R-EGFP (green) was used as a MAM marker. The lower left panel displays the merged image of Pml and Sigma 1-R staining. The lower right panel displays the Pml signal overlaid with MAMs (MAM boundaries are highlighted in yellow) in a rainbow LUT ($MAMs_{PML}$: Manders coefficient for Pml staining was calculated according to Manders coefficient method as the proportion of Pml signal overlapping with the Sigma 1-R marker). Scale bar, 10 μm

(F-G) Detection of autophagy induction in $p53^{-/-}$ MEFs following the re-introduction of $p53^{wt}$ or mutant $p53^{K382R}$ based on GFP-LC3 puncta. Representative images are shown in (F) Bars: S.E.M. ** $p < 0.01$, n=4. Scale bar, 10 μm.

(H) Immunofluorescence of Pml (red) and p53 (blue) in $p53^{-/-}$ MEFs after the re-introduction of mutant $p53^{K382R}$. Sigma 1-R-EGFP (green) was used as a MAM marker. The lower left panel displays the merged image of Pml and Sigma 1-R staining. The lower right panel displays the Pml signal overlaid with MAMs (MAM boundaries are highlighted in yellow) in a rainbow LUT ($MAMs_{PML}$: Manders coefficient for Pml staining was calculated according to Manders coefficient method as the proportion of Pml signal overlapping with the Sigma 1-R marker). Scale bar, 10 μm.

(I) Representative images of PLA (red signal) from H1299 cells reintroduced of $p53^{wt}$ or $p53^{K382R}$. Sigma 1-R-EGFP (green) was used as a MAMs marker. Scale bar, 10 μm. On the bottom left panel zoomed regions display interaction sites in close contacts with Sigma 1-R-EGFP dots (scale bar, 2 μm). On upper right panel, quantitative analysis of PLA signal between PML and $p53^{wt}$ or $p53^{K382R}$. Bars: S.E.M. **** $p < 0.001$. n=3.

Figure S4

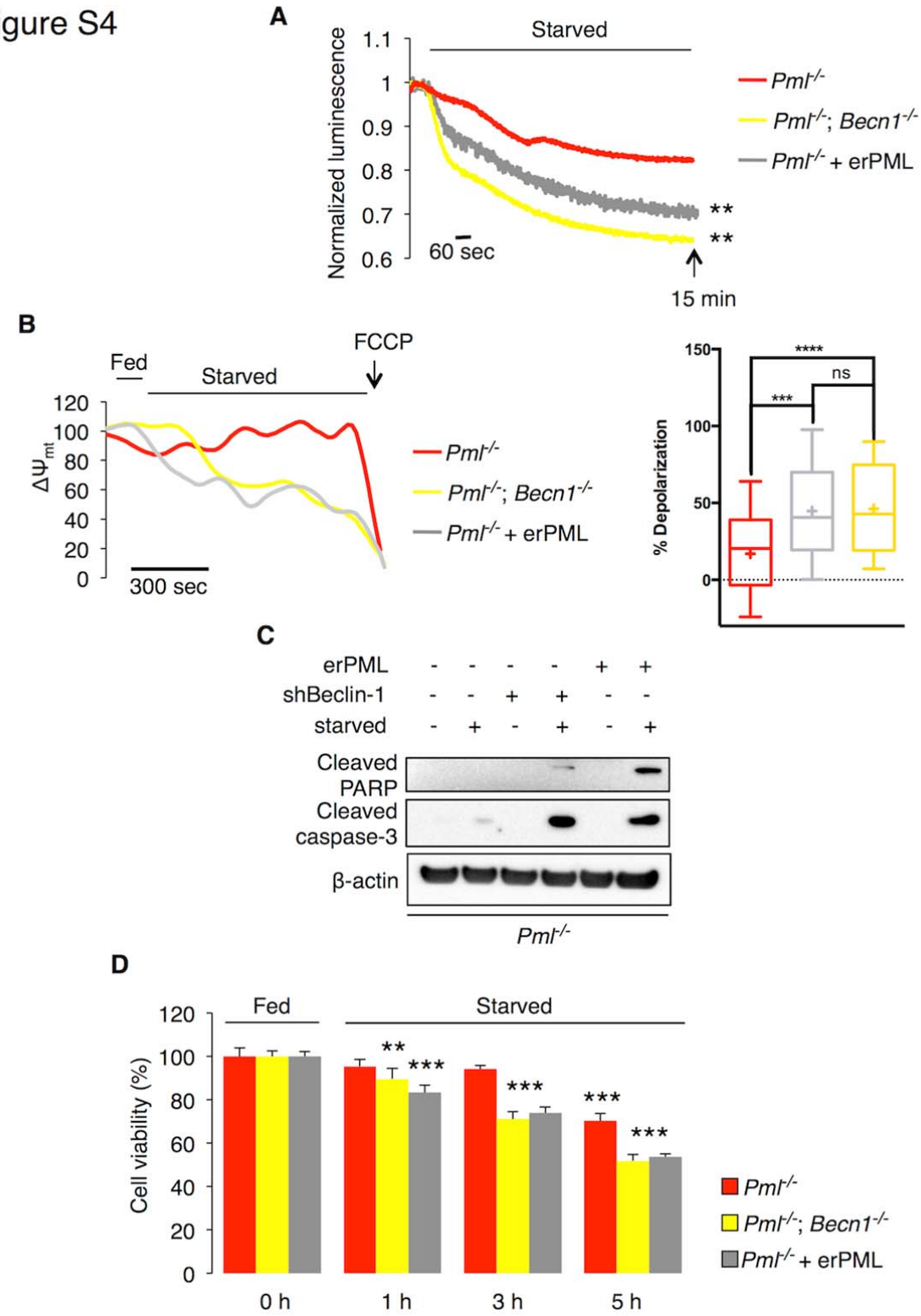
A
Starved
Normalized luminescence
1.1
1
0.9
0.8
0.7
0.6
60 sec
15 min
**
**
Pml-/-
Pml-/-; Becn1-/-
Pml-/- + erPML
B
Fed
Starved
FCCP
ΔΨmt
120
100
80
60
40
20
0
300 sec
Pml-/-
Pml-/-; Becn1-/-
Pml-/- + erPML
% Depolarization
150
100
50
0
****
ns
***
C
erPML - - - - + +
shBeclin-1 - - + + - -
starved - + - + - +
Cleaved PARP
Cleaved caspase-3
β-actin
Pml-/-
D
Fed
Starved
Cell viability (%)
120
100
80
60
40
20
0
**
***
***
***
***
0 h
1 h
3 h
5 h
Pml-/-
Pml-/-; Becn1-/-
Pml-/- + erPML

Figure S4, Related to Figure 5. Inhibition of autophagy in PML KO cells confers sensitivity to metabolic stress.
(A) Cytosolic ATP levels in MEFs *Pml*$^{-/-}$, *Pml*$^{-/-}$;*Becn1*$^{-/-}$ and *Pml*$^{-/-}$ after re-introduction of erPML chimera as measured by luciferase expression under starvation conditions (glucose deprivation for 15 min). ** $p < 0.01$, compared to KO condition, n=3.
(B) Analysis of mitochondrial membrane potential (Ψ_m) as measured by TMRM intensity in MEFs *Pml*$^{-/-}$, *Pml*$^{-/-}$; *Becn1*$^{-/-}$ and *Pml*$^{-/-}$ after re-introduction of erPML chimera. Where indicated, cells were deprived of glucose or exposed to 1 μM carbonyl cyanide p-trifluoromethoxyphenylhydrazone (FCCP). (statistical analysis cross: average, line: median, box: 25 and 75 percentile, bars: max and min value, *** $p < 0.005$, n = 3).
(C) Susceptibility to cell death and (D) cell viability of MEFs *Pml*$^{-/-}$, *Pml*$^{-/-}$; *Becn1*$^{-/-}$ and *Pml*$^{-/-}$ after re-introduction of erPML chimera under stress condition induced by glucose deprivation (3 h for western blot and the indicated hours for cell viability). Bars: S.E.M. ** $p < 0.01$, *** $p < 0.005$, n=3.

Figure S5

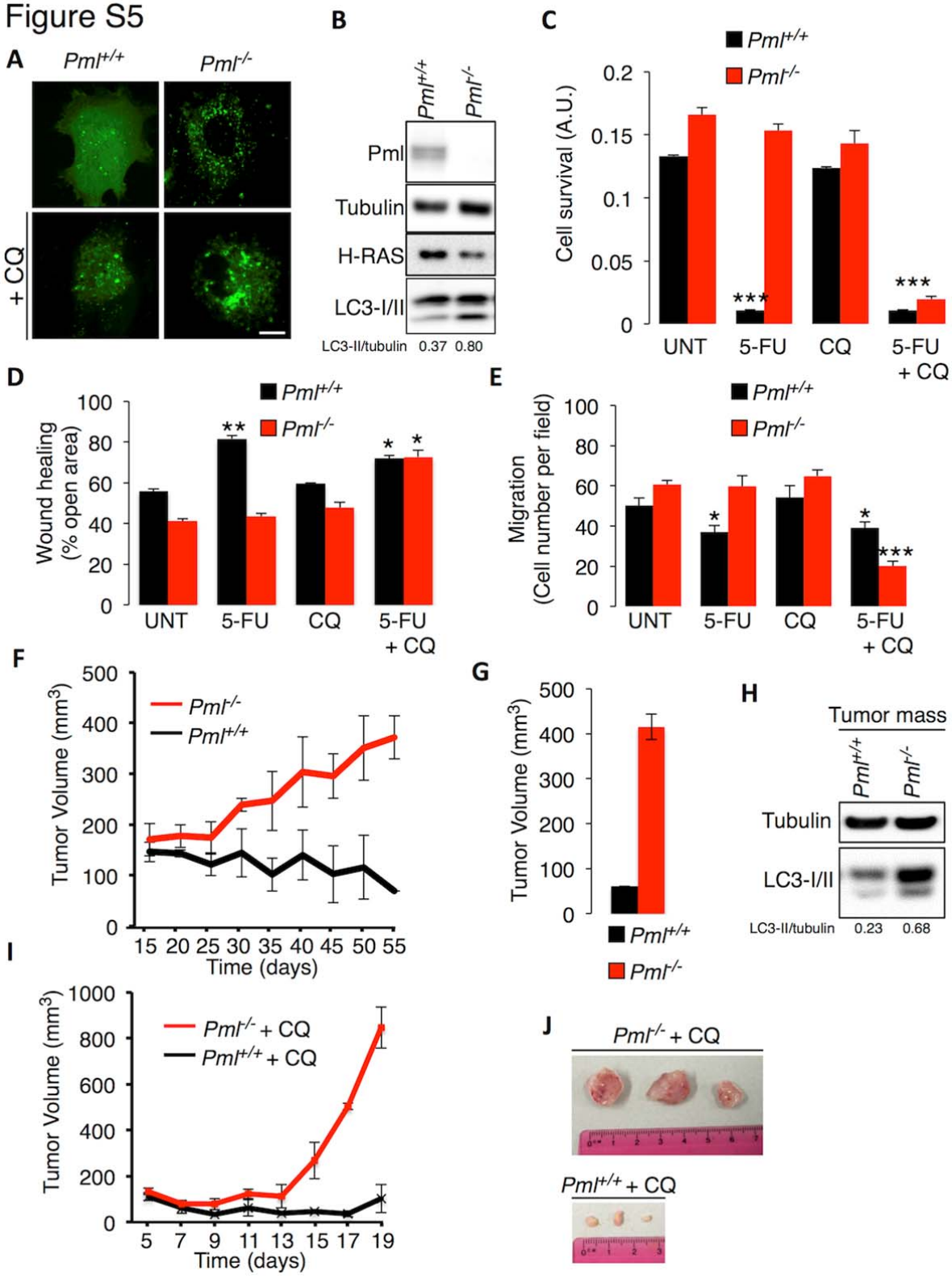
A
Pml+/+
Pml-/-
+ CQ
B
Pml+/+
Pml-/-
Pml
Tubulin
H-RAS
LC3-I/II
LC3-II/tubulin 0.37 0.80
C
Pml+/+
Pml-/-
Cell survival (A.U.)
0.2
0.15
0.1
0.05
0
***
***
UNT
5-FU
CQ
5-FU + CQ
D
Pml+/+
Pml-/-
Wound healing (% open area)
100
80
60
40
20
0
**
*
*
UNT
5-FU
CQ
5-FU + CQ
E
Pml+/+
Pml-/-
Migration (Cell number per field)
100
80
60
40
20
0
*
*
***
UNT
5-FU
CQ
5-FU + CQ
F
Pml-/-
Pml+/+
Tumor Volume (mm3)
500
400
300
200
100
0
15 20 25 30 35 40 45 50 55
Time (days)
G
Tumor Volume (mm3)
500
400
300
200
100
0
Pml+/+
Pml-/-
H
Tumor mass
Pml+/+
Pml-/-
Tubulin
LC3-I/II
LC3-II/tubulin 0.23 0.68
I
Pml-/- + CQ
Pml+/+ + CQ
Tumor Volume (mm3)
1000
800
600
400
200
0
5 7 9 11 13 15 17 19
Time (days)
J
Pml-/- + CQ
Pml+/+ + CQ

Figure S5, Related to Figure 7. Tumorigenic potential of *Pml*$^{-/-}$- and *Pml*$^{+/+}$- transformed MEFs.
(A) Representative images of LC3 puncta accumulation after CQ treatments in MEF cells. Scale bar, 10 μm.
(B) Analysis of autophagy in *Pml*$^{+/+}$ and *Pml*$^{-/-}$ transformed MEFs.
(C) Cell proliferation of *Pml*$^{+/+}$- and *Pml*$^{-/-}$-transformed MEFs as analyzed by crystal violet staining (absorbance at 595 nm) in the presence of various treatments (5-FU at 25 μM, CQ at 5 μM or 5-FU at 25 μM and CQ at 5 μM, for 24 h). Bars: S.E.M. *** $p < 0.005$ compared to untreated condition (UNT), n=3.
(D) *Pml*$^{-/-}$- transformed MEFs showed reduced wound-healing ability compared with that of *Pml*$^{+/+}$ cells (5-FU at 25 μM, CQ at 5 μM or 5-FU at 25 μM and CQ at 5 μM, 24 h). Bars: S.E.M. * $p < 0.05$, ** $p < 0.01$, compared to untreated condition (UNT), n=3.
(E) Quantification of *Pml*$^{+/+}$- and *Pml*$^{-/-}$-transformed MEF migration in the presence of various treatments (5-FU at 25 μM, CQ at 5 μM or 5-FU at 25 μM and CQ at 5 μM, 24 h). Bars: S.E.M. * $p < 0.05$, *** $p < 0.005$, compared to untreated condition (UNT), n=3.
(F) Pml+/+ sv129 mice were inoculated with Pml+/+- and Pml-/--transformed MEFs. Tumor growth was analyzed at different time points. After 55 days from inoculation tumors were excised and tumor volume (G) was measured. In parallel, the lipidation of LC3-I into the autophagic form LC3-II was assessed by immunoblot (H). Bars: S.E.M.
(I) Analysis of tumor growth following the inoculation of *Pml*$^{+/+}$- and *Pml*$^{-/-}$-transformed MEFs into nude/nude mice treated with CQ (60 mg/kg) and (J) representative images of tumors excised on day 19 after inoculation.

Figure S6

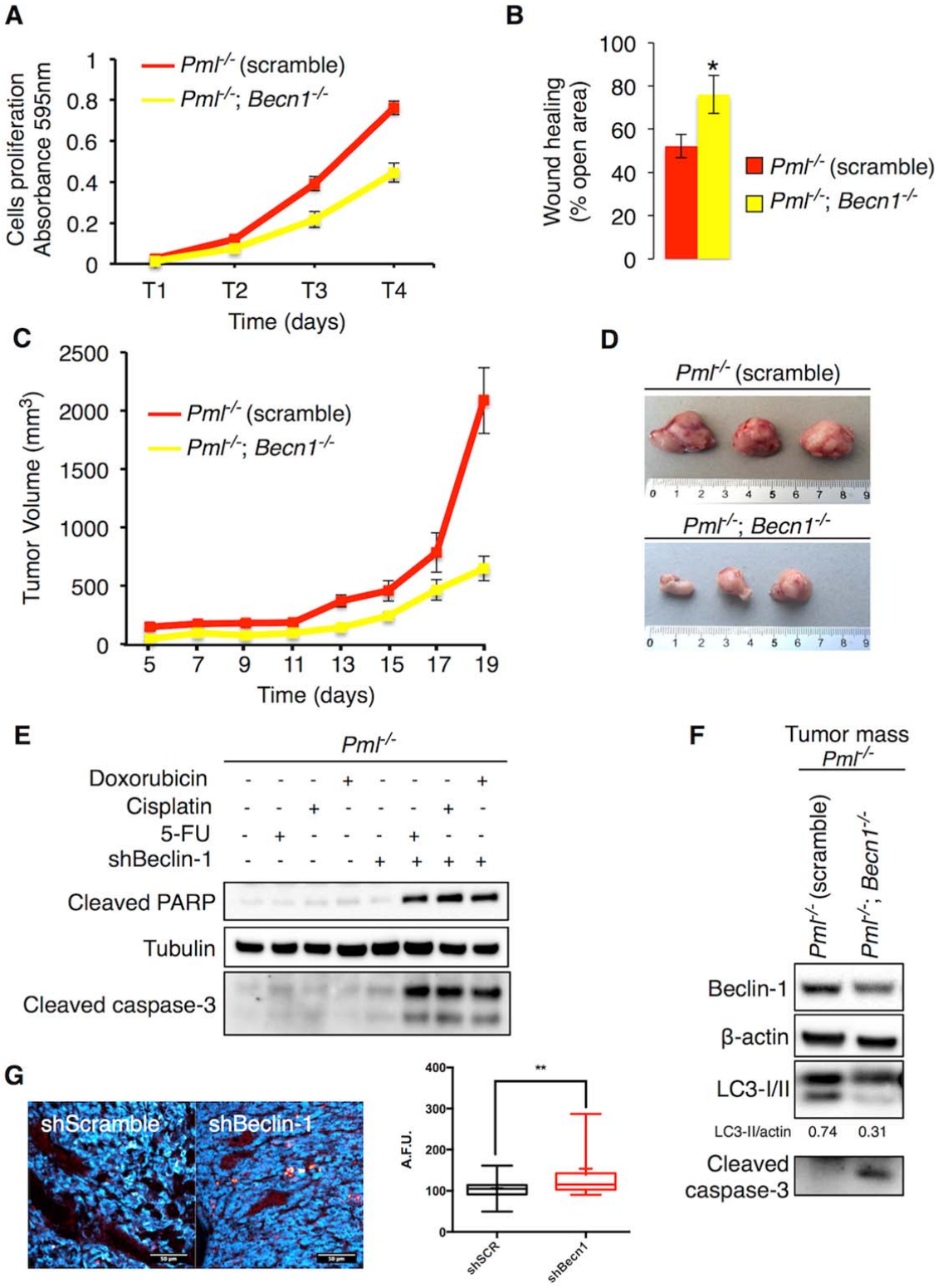
A
Cells proliferation Absorbance 595nm
Pml-/- (scramble)
Pml-/-; Becn1-/-
Time (days)
T1
T2
T3
T4
B
Wound healing (% open area)
*
Pml-/- (scramble)
Pml-/-; Becn1-/-
C
Tumor Volume (mm3)
Pml-/- (scramble)
Pml-/-; Becn1-/-
Time (days)
D
Pml-/- (scramble)
Pml-/-; Becn1-/-
E
Pml-/-
Doxorubicin
Cisplatin
5-FU
shBeclin-1
Cleaved PARP
Tubulin
Cleaved caspase-3
F
Tumor mass
Pml-/-
Pml-/- (scramble)
Pml-/-; Becn1-/-
Beclin-1
β-actin
LC3-I/II
LC3-II/actin 0.74 0.31
Cleaved caspase-3
G
shScramble
shBeclin-1
A.F.U.
**
shSCR
shBecn1

Figure S6, Related to Figure 7. Genetic inhibition of autophagy triggers apoptosis and delays tumor growth in the absence of PML.

(A) Cell proliferation of *Pml*$^{-/-}$ (scramble shRNA) and *Pml*$^{-/-}$ silenced for Beclin-1 (*Pml*$^{-/-}$; *Becn1*$^{-/-}$) MEFs as analyzed by crystal violet staining (absorbance at 595 nm).

(B) Wound-healing assay of MEFs Pml-/- (scramble shRNA) and Pml-/- silenced for Beclin-1 (Pml-/-; Becn1-/-). Bars: S.E.M. * $p < 0.05$.

(C) Tumor growth of *Pml*$^{-/-}$ (scramble shRNA) and *Pml*$^{-/-}$ silenced for Beclin-1 (*Pml*$^{-/-}$; *Becn1*$^{-/-}$) transformed MEF xenografts and respectively (D) representative images.

(E) Sensitivity to apoptosis induced by different chemotherapeutic agents (5-FU, Doxorubicin and cisplatin 10 μM, 6 h) in MEFs *Pml*$^{-/-}$ and *Pml*$^{-/-}$;*Becn1*$^{-/-}$.

(F) Analysis of autophagy and apoptosis by immunoblot of tumor tissues.

(G) Analysis of apoptosis based on the intensity of fluorescence (SR-FLIVO) emitted in tumor tissue sections, accompanied by statistical analysis. (cross: average, line: median, box: 25 and 75 percentile, bars: max and min value, *** $p < 0.005$, $n = 3$). Scale bar, 50 μm.

SUPPLEMENTAL EXPERIMENTAL PROCEDURES

Cell culture and transfection

Primary *Pml*$^{+/+}$ and *Pml*$^{-/-}$ mouse embryonic fibroblasts (MEFs) were prepared from embryos at day 13.5 of development (E13.5). Early passage (P2–P5) MEFs and H1299 cells were cultured in Dulbecco's modified Eagle's medium (DMEM) supplemented with 10% fetal bovine serum (FBS) (Life Technologies), 100 U/ml penicillin (EuroClone), 100 mg/ml streptomycin (EuroClone) and 4 mM L-glutamine (EuroClone).
Human APL NB4 cells were cultured in RPMI 1640 medium (Gibco) supplemented with 10% FBS (Gibco) and 1% penicillin-streptomycin-glutamine (100×) liquid (Gibco).
All cells were maintained at 37°C in a humidified atmosphere of 5% CO_2.
MEFs were transformed with SV40 large T antigen. MEFs were transfected with the following plasmids: PML, erPML, nuPML (Giorgi et al., 2010), p53^{WT}, p53^{K382R} (Morselli et al., 2011), MCU (De Stefani et al., 2011) and GFP-LC3 using a MicroPorator (Digital Bio). For PML depletion in WT MEFs, a specific shRNA silencing lentiviral vector (Sigma) was used. H1299 cells were transfected using a standard calcium phosphate procedure with p53^{WT} and p53^{K382R} constructs, while NB4 cells were transfected with a GFP-LC3 plasmid by electroporation.

Autophagy induction, inhibition and analysis of autophagic flux

After treatment, the cells were fixed or lysed to detect the amount of autophagosome vesicles by fluorescence microscopy (with the employment of the GFP-LC3 plasmid) or by immunoblot analysis (using LC3 antibody) (Klionsky et al., 2016; Mizushima et al., 2010).
For genetic inhibition of autophagy, we generated clones stably expressing shRNA beclin1 by culturing transfected cells in the presence of zeocin (500 μg/ml, added 48 h after transfection) for 3 weeks. Stable shRNABeclin1 clones were kept in the continuous presence of 50 μg/ml zeocin (Invitrogen).
For *in vivo* studies on the effects of starvation, mice were deprived of food for 24 h. The mice had free access to drinking water. For determination of autophagic flux *in vivo,* lysosomal activity was blocked by intraperitoneal administration of 40 mg/kg body weight of leupeptin (Sigma) in saline solution. Control animals were injected with an equivalent volume of saline solution. 4 h after injection the animals were euthanized and the livers isolated (Boya et al., 2005). After euthanasia mice tissues were processed and immunoblotted.

Quantitative analysis of GFP-LC3 dots

Pml$^{+/+}$ and *Pml*$^{-/-}$ MEFs were transfected as follows: *Pml*$^{+/+}$ and *Pml*$^{-/-}$ MEFs: 2 μg pcDNA3 + 1 μg GFP-LC3; *Pml*$^{-/-}$ MEFs expressing nuPML: 2 μg nuPML + 1 μg GFP-LC3; *Pml*$^{-/-}$ MEFs expressing erPML: 2 μg erPML + 1 μg GFP-LC3; *Pml*$^{-/-}$ MEFs expressing MCU: 2 μg MCU + 1 μg GFP-LC3.
p53$^{-/-}$ MEFs were transfected as follows: p53$^{-/-}$ MEFs: 2 μg *pcDNA3* + 1 μg GFP-LC3; p53$^{-/-}$ MEFs expressing erPML: 2 μg erPML + 1 μg GFP-LC3; p53^{WT}-overexpressing cells: 2 μg p53^{WT} + 1 μg GFP-LC3; p53^{K382R}-overexpressing cells: 2 μg p53^{K382R} + 1 μg GFP-LC3.
NB4 were transfected with 3μg GFP-LC3.

Aequorin measurements

Primary *Pml*$^{-/-}$ MEFs were transfected with the appropriate aequorin chimera targeted to the mitochondria (mtAEQmut) (Bonora et al., 2013) alone or together with MCU expression constructs as follows: *Pml*$^{-/-}$ MEFs: 0.75 μg pcDNA3 + 0.25 μg mtAEQmut; *Pml*$^{-/-}$ MEFs expressing MCU: 0.75 μg MCU + 0.25 μg mtAEQmut. All aequorin measurements were performed in Krebs-Ringer buffer (KRB) supplemented with 1 mM $CaCl_2$. An agonist was added to the same medium as specified in the figure legends. The experiments were terminated by lysing the cells with 100 μM digitonin in a hypotonic Ca^{2+}-rich solution (10 mM $CaCl_2$ in H_2O), thus discharging the remaining aequorin pool. The light signal was collected and calibrated into [Ca^{2+}] values, as described previously (Pinton et al., 2007).

Luciferase measurements

Primary *Pml*$^{+/+}$ and *Pml*$^{-/-}$ MEFs were transfected with cytosolic (untargeted) firefly luciferase (Jouaville et al., 1999). Cell luminescence was measured in the same luminometer used for the aequorin measurements with constant perfusion of KRB supplemented with 1 mM $CaCl_2$ and 20 μM luciferin for 60 sec. Then, the cells were perfused with glucose-free KRB supplemented with 1 mM $CaCl_2$ and 20 μM luciferin for 15 min. The light output of a coverslip of transfected cells was in the range of 1,000–10,000 counts per second (cps) *versus* the background at 10 cps.

Cell proliferation and viability assay, wound healing and migration assay

For the proliferation and viability assay the data are presented as a histogram showing the percentage of the cell number referred to the control condition.
For wound healing assay the cells were monitored and captured by phase-contrast microscopy (a Leica phase-contrast microscope equipped with an ICC50 HD camera and a 4X objective). Then, the percentage of the open scratched area

was measured using the Wound Healing Tool available in the software Fiji. Five replicates each of three independent experiments were performed.
For migration assay the average number of migrating cells was calculated from the total number of cells counted per chamber using the Cell Counter plugin available in the software ImageJ.

Western blot
Total cell lysates were prepared in RIPA buffer (50 mM Tris-HCl [pH 7.8], 150 mM NaCl, 1% IGEPAL CA-630, 0.5% sodium deoxycholate, 0.1% SDS, and 1 mM dithiothreitol [DTT]) supplemented with proteases and phosphatase inhibitors (2 mM Na_3VO_4, 2 mM NaF, 1 mM PMSF and protease inhibitor cocktail). In total, 20 μg protein was separated by SDS/PAGE and transferred to nitrocellulose membranes for standard western blot analysis.
The following antibodies was used: PML anti-mouse (1:1000) from Chemicon (Merck Millipore, Billerica, MA, USA); β-actin (1:3000), β-tubulin (1:3000), MCU (1:1000), p62 (1:3000), Sigma 1-R (1:1000) and STX17 (1:1000) from Sigma-Aldrich (Saint Louis, MO, USA); Atg14 (1:500) from MBL (Woburn, MA); IP3R3 (1:1000) and Cyt *c* (1:10000) from BD Biosciences (San Jose, CA, USA); ACC (1:1000), P-ACC (1:1000), AMPK (1:1000), P-AMPK (1:1000), Beclin-1 (1:1000), Caspase-3 (1:500), GAPDH (1:6000), LC3-B (1:1000), mTOR (1:1000), P-mTOR (1:1000), mouse-p53 (1:1000), p70S6 Kinase (1:1000), P-p70S6 kinase (1:1000), PARP (1:1000), ULK1 (1:1000) and P-ULK1^{Ser317} (1:1000) from Cell Signaling (Danvers, MA, USA); p53 DO-1 (1:500) and PML anti-human (1:500) from Santa Cruz (Santa Cruz, CA, USA); H-RAS antiserum (1:1000) from Novus Biologicals (Littleton, CO, USA); RARα (1:1000) from abcam (Cambridge, UK).
Isotype-matched horseradish peroxidase-conjugated secondary antibodies were used, followed by detection using chemiluminescence (PerkinElmer, Waltham, MA, USA).

Immunofluorescence assay
MEFs or H1299 were co-transfected with a plasmid coding for Sigma-1R-EGFP or SEC61b-EGFP or 4mt-Cherry and a plasmid for p53^{WT}, p53^{K382R} or PML according to experiment. Next, at 36 h after transfection, the cells were fixed in 3.7% formaldehyde in PBS for 20 min and washed three times with PBS. Formaldehyde autofluorescence was quenched by Glycine 100mM in HBSS pH 8.5 for 10 min at RT. Permeabilization of cell membranes was accomplished by 10 min incubation with 0.1% Triton X-100 in PBS, followed by a 1 h blocking with 2% bovine serum albumin (BSA) in PBS. MEFs were incubated overnight at 37°C in a wet chamber with rabbit anti-PML antibody (Abcam) and mouse anti-p53 antibody (Cell Signaling) diluted 1:100 with 2% BSA in PBS. H1299 were incubated overnight at 37°C in a wet chamber with mouse anti-PML antibody (Abcam) and rabbit anti-PDI antibody (Abcam) or rabbit anti Sigma1R (Sigma Aldrich) or mouse anti p53 (Santa Cruz) diluted 1:100 with 2% BSA in PBS. Then, staining was performed with Alexa 633 goat anti-mouse or Alexa 546 goat anti-rabbit or Alexa 488 goat anti-rabbit secondary antibodies, according to experiment. After antibody incubation, the cells were washed four times with PBS. Images were acquired using an LSM 510 laser scanning confocal microscope (Zeiss) equipped with 63X oil immersion objectives (N.A. 1.4, Zeiss) with a final pixel size of 140 nm. The pinhole size was set to allow Z sections of 1 μm thickness. Visualization of PML on MAMs was performed by overlaying the boundaries of MAM regions onto the PML signal. MAM region boundaries were obtained by thresholding the Sigma-1R-EGFP signal and converting the edges of the thresholded signal to regions of interest using the Analyze particles tool in the open source software Fiji (available at http://fiji.sc/Fiji). Then, the MAM boundaries were overlaid onto the image of the PML signal that was converted previously to a rainbow LUT. This process allowed the visualization of both weak and strong signals. All image processing was performed using the open source software Fiji. Colocalization between PML and PDI or SIGMA1R or SEC61B-EGFP or SIGMA1R-EGFP was performed using the Co-localization Threshold plugin

Measurements of mitochondrial membrane potential (Ψ_m)
Ψ_m was assessed by loading cells with 10 nM tetramethyl rhodamine methyl ester (TMRM; Life Technologies, T-668) for 35 min at 37°C in KRB supplemented with 1 mM $CaCl_2$. Images were acquired using an inverted microscope (Nikon LiveScan Swept Field Confocal Microscope Eclipse Ti equipped with NIS-Elements microscope imaging software and 40X oil immersion lens, Nikon Instruments). TMRM excitation was performed at 560 nm, and emission was collected through a 590 to 650 nm band-pass filter. After 2 min, KRB medium was exchanged with KRB without glucose. Images were acquired every 30 sec with a fixed 20 ms exposure time. FCCP (carbonyl cyanide p-trifluoromethoxyphenylhydrazone, 10 μM), an uncoupler of oxidative phosphorylation, was added after 30 acquisitions to completely collapse the electrical gradient established by the respiratory chain.
To correct TMRM signal upon oscillation induce by temperature and solution changes mitochondrial signal were normalized according to total and mitochondrial TMRM amount relationship published in (Scaduto and Grotyohann, 1999). Total and mitochondrial TMRM signal where obtained by differential thresholding before and after FCCP administration. Kinetics with stable basal value were considered correctly calibrated. Glucose deprivation induced depolarization was calculated as the reduction in TMRM signal after 20 min of glucose deprivation.

Pre-embedding immunogold electron microscopy
Cells were fixed with 4% formaldehyde in 0.1 M phosphate buffer (pH 7.4) for 1 h at room temperature. Cells were washed in PBS and treated with 50 mM glycine for 10 min. Subsequently, cells were permeabilized with 0.25%

saponin, 0.1% BSA and blocked in blocking buffer for 30 min. Cells were incubated sequentially with PML primary antibodies (Millipore MAB3738 or abcam ab72137) and goat anti-mouse or goat anti-rabbit nanogold-conjugated secondary antibodies (Nanoprobes) diluted in blocking buffer. After washes in PBS, cells were re-fixed in 1% glutaraldehyde, and nanogold was enlarged with gold enhancement solution (Nanoprobes) according to the manufacturer's instructions. Cells were post-fixed with osmium tetroxide, embedded in epon and processed into ultrathin slices. After contrasting with uranyl acetate and lead citrate, sections were analyzed with a Zeiss LEO 512 electron microscope. Images were acquired by a 2k x 2k bottom-mounted slow-scan Proscan camera controlled by EsivisionPro 3.2 software.

Migration assay

In vitro cell migration assays were performed using Costar Transwell permeable polycarbonate supports (8.0 mm pores) in 24-well plates (Corning Inc.). Before seeding (1×10^5 *Pml* $^{+/+}$ and *Pml* $^{-/-}$ MEFs), the lower compartment was incubated with DMEM plus 10% FBS supplemented with vehicle (positive control), 25 μM 5-FU, 5 μM CQ or 25 μM 5-FU and 5 μM CQ. Non-migrated cells were removed using a cotton swab, and migrated cells were fixed and stained with crystal violet. The migratory cells of five fields were imaged under a Leica phase-contrast microscope equipped with an ICC50 HD camera and a 4X objective.

Immunoelectron microscopy

H1299 *p53*$^{-/-}$ cells and H1299 after the re-introduction of p53^{wt} were fixed in 2% paraformaldehyde and 0.2% glutaraldehyde in phosphate-buffered saline (PBS), embedded in 12% gelatin and 2.3 M sucrose and frozen in liquid nitrogen. Ultrathin cryo-sections, obtained using a Reichert-Jung Ultracut E with a FC4E cryoattachment, were collected on copper-formvar-carbon-coated grids. Immunogold localization was revealed using PML antibody for endogenous human Pml (Abcam) and conjugated 10 nm protein A-gold according to published protocols (Confalonieri et al., 2000; Slot et al., 1991). All samples were examined using a Philips CM10 or a FEI Tecnai 12G2 electron microscope.

Mouse treatment studies

Procedures involving animals and their care were in conformity with institutional guidelines, and all experimental protocols were approved by the Animal Ethics Committee.

Pml$^{+/+}$ and *Pml*$^{-/-}$ sv129 mice were housed in a temperature-controlled environment with 12 h light/dark cycles and received food and water *ad libitum*.

Seven-weeks-old female athymic mice (Balb/c *nu/nu*, Harlan) were housed and handled under aseptic conditions for xenografts tumors, while seven-weeks-old female sv129 mice were used for syngeneic tumors.

Tumor volumes were measured every other day for xenograft tumors and every 5 days for syngeneic tumors with calipers using the following equation: $Volume = \pi/6 \times (a \times b^2)$, where a is the major diameter and b is the minor diameter. The athymic mice were divided into the treatment groups and the control group, with 10 mice per group. After five days, the treatments were initiated as follows: (a) PBS group, animals received intraperitoneal (i.p.) injections of 100 μl PBS every day; (b) 5-FU group, animals received i.p. injections of 30 mg/kg 5FU in 100 μl PBS twice weekly; (c) 5-FU + chloroquine (CQ) group, animals received i.p. injections of 30 mg/kg 5-FU twice weekly and 60 mg/kg CQ in 100 μl PBS every day; and (d) CQ group, animals received i.p. injections of 60 mg/kg CQ in 100 μl PBS every day. After 2 weeks of treatment, all mice were sacrificed, and tumors were immunoblotted. Sv129 mice were sacrificed after 55 days and tumors were immunoblotted.

Tissue processing

Pml$^{+/+}$ and *Pml*$^{-/-}$ mice were bred and maintained according to both the Federation for Laboratory Animal Science Associations and the Animal Experimental Ethics Committee guidelines.

For studies on the effects of starvation, mice were deprived of food for 24 h. The mice had free access to drinking water. After killing the mice, their livers were homogenized in 20 mM Tris buffer (pH 7.4) containing 150 mM NaCl, 1% Triton X-100, 10 mM EDTA and protease inhibitor cocktail. Then, tissue extracts were centrifuged at 12,000 × g at 4°C for 10 min. Finally, protein extracts (20 μg each) were subjected to SDS-PAGE and immunoblotting.

Mouse muscles were ground by mortar and pestle and lysed in a buffer containing 50 mM Tris (pH 7.5), 150 mM NaCl, 10 mM $MgCl_2$, 0.5 mM DTT, 1 mM EDTA, 10% glycerol, 2% SDS, 1% Triton X-100, Roche Complete Protease Inhibitor Cocktail, 1 mM PMSF, 1 mM $NaVO_3$, 5 mM NaF and 3 mM β-glycerophosphate. Then, tissue extracts were centrifuged at 12,000 × g at 4°C for 10 min. Finally, protein extracts (20 μg each) were subjected to SDS-PAGE and immunoblotting.

Mice tumors were excised and homogenized in lysis buffer (300 mM sucrose, 1 mM K_2HPO_4, 5.5 mM D-glucose, 20 mM Hepes, 1 mM phenylmethylsulfonylfluoride, and 0.5% IGEPAL) with a Potter pestle. Then, were centrifuged at 12,000 × g at 4°C for 15 min. Finally, protein extracts (20 μg each) were subjected to SDS-PAGE and immunoblotting.

Detection of cell death *in vivo*

After staining, the samples were mounted on coverslips and analyzed using a Zeiss LSM 510 confocal microscope equipped with an objective Fluor 40X/1.30 Oil. Images were background corrected, and signals were analyzed using open source Fiji software (available at http://fiji.sc/Fiji).

XF bioenergetic analysis

OCRs in *Pml*$^{+/+}$ and *Pml*$^{-/-}$ MEFs were measured using a Seahorse XF96 instrument (Seahorse Biosciences, North Billerica, MA) according to the manufacturer's protocols. MEFs were seeded in a XF96 microplate at a density of 15,000 cells per well and allowed to attach. The following day, the medium was exchanged, where indicated, with 175 µl unbuffered XF assay media at pH 7.4 (Seahorse Biosciences) supplemented with 5.5 mM glucose (Sigma), 1 mM sodium pyruvate and 1 mM glutamine or with 175 µl unbuffered XF assay media at pH 7.4 (Seahorse Biosciences) without glucose, sodium pyruvate or glutamine. Then, the microplate was placed in a 37°C non-CO_2 incubator for 60 min. Respiration was measured in four blocks of three for 3 min each. The first block measured the basal respiration rate. Next, 1 µm oligomycin (Seahorse Biosciences, North Billerica, MA) was added to inhibit complex V, and the second block was measured. Then, 1 µm FCCP (Seahorse Biosciences, North Billerica, MA) was added to uncouple respiration, and the third block was measured. Finally, 1 µm antimycin A (Seahorse Biosciences, North Billerica, MA) and 1 µm rotenone (Seahorse Biosciences, North Billerica, MA) were added to inhibit complex III, and the last measurements were performed. Immediately after finishing the measurements, the cells were washed with PBS, fixed in 4% paraformaldehyde and stained with 0.1% crystal violet. Crystal violet was dissolved with 1 mol/l acetic acid, and absorbance at 595 nm was measured as an index of cell amount.

Proximity Ligation Assay

p53$^{+/+}$ and *p53*$^{-/-}$ MEFs were transfected using microporator with plasmid coding for SIGMA1R-EGFP and seeded on microarray slide 16-well (thermo Fisher) at density of 20000 and 15000 respectively. Twenty-four hours after seeding cells were hybridized with antibody for PML and p53 according to the immunostaining procedure. The day after samples were hybridized with PLUS and MINUS probes blocked with goat serum 2.5% and BSA 2.5% in PBS for 30 minutes at room temperature. Proximity ligation assay was then concluded according to manufacturer instruction. PLA signal was detected by a Olympus Xcellence widefield system, and deconvolved using Fiji. After 3D digital deconvolution PLA signal was quantified as the integrated signal of each SIGMA 1-R-EGFP positive cell.

SUPPLEMENTAL REFERENCES

Bonora, M., Giorgi, C., Bononi, A., Marchi, S., Patergnani, S., Rimessi, A., Rizzuto, R., and Pinton, P. (2013). Subcellular calcium measurements in mammalian cells using jellyfish photoprotein aequorin-based probes. Nat Protoc 8, 2105-2118.

Boya, P., Gonzalez-Polo, R. A., Casares, N., Perfettini, J. L., Dessen, P., Larochette, N., Metivier, D., Meley, D., Souquere, S., Yoshimori, T., et al. (2005). Inhibition of macroautophagy triggers apoptosis. Mol Cell Biol 25, 1025-1040.

Confalonieri, S., Salcini, A. E., Puri, C., Tacchetti, C., and Di Fiore, P. P. (2000). Tyrosine phosphorylation of Eps15 is required for ligand-regulated, but not constitutive, endocytosis. J Cell Biol 150, 905-912.

De Stefani, D., Raffaello, A., Teardo, E., Szabo, I., and Rizzuto, R. (2011). A forty-kilodalton protein of the inner membrane is the mitochondrial calcium uniporter. Nature.

Esteban-Martinez, L., and Boya, P. (2015). Autophagic flux determination in vivo and ex vivo. Methods 75, 79-86.

Giorgi, C., Ito, K., Lin, H. K., Santangelo, C., Wieckowski, M. R., Lebiedzinska, M., Bononi, A., Bonora, M., Duszynski, J., Bernardi, R., et al. (2010). PML regulates apoptosis at endoplasmic reticulum by modulating calcium release. Science 330, 1247-1251.

Jouaville, L. S., Pinton, P., Bastianutto, C., Rutter, G. A., and Rizzuto, R. (1999). Regulation of mitochondrial ATP synthesis by calcium: evidence for a long-term metabolic priming. ProcNatlAcadSciUSA 96, 13807-13812.

Klionsky, D. J., Abdelmohsen, K., Abe, A., Abedin, M. J., Abeliovich, H., Acevedo Arozena, A., Adachi, H., Adams, C. M., Adams, P. D., Adeli, K., et al. (2016). Guidelines for the use and interpretation of assays for monitoring autophagy (3rd edition). Autophagy 12, 1-222.

Mizushima, N., Yoshimori, T., and Levine, B. (2010). Methods in mammalian autophagy research. Cell 140, 313-326.

Morselli, E., Shen, S., Ruckenstuhl, C., Bauer, M. A., Marino, G., Galluzzi, L., Criollo, A., Michaud, M., Maiuri, M. C., Chano, T., et al. (2011). p53 inhibits autophagy by interacting with the human ortholog of yeast Atg17, RB1CC1/FIP200. Cell Cycle 10, 2763-2769.

Pinton, P., Rimessi, A., Romagnoli, A., Prandini, A., and Rizzuto, R. (2007). Biosensors for the detection of calcium and pH. Methods Cell Biol 80, 297-325.

Scaduto, R. C., Jr., and Grotyohann, L. W. (1999). Measurement of mitochondrial membrane potential using fluorescent rhodamine derivatives. Biophys J 76, 469-477.

Slot, J. W., Geuze, H. J., Gigengack, S., Lienhard, G. E., and James, D. E. (1991). Immuno-localization of the insulin regulatable glucose transporter in brown adipose tissue of the rat. J Cell Biol 113, 123-135.